PROCEEDINGS OF SCIENCE

Measurements of Higgs boson couplings and simplified template cross sections in bosonic final states (WW^*, ZZ^*, $\gamma\gamma$) at the ATLAS experiment

Theodota Lagouri * **on behalf of the ATLAS Collaboration**

Yale University,
New Haven, CT, US
E-mail: theodota.lagouri@cern.ch

The Higgs boson decays to bosons provide very detailed measurements of Higgs boson properties and interactions, and shine light on the mechanism of electroweak symmetry breaking. This paper presents the latest measurements of the Higgs boson coupling properties performed by the ATLAS experiment in various bosonic decay channels (WW^*, ZZ^* and $\gamma\gamma$) using the full Run-2 p-p collision dataset collected at $\sqrt{s}$=13 TeV with luminosity of 139 fb^{-1}. Results on production mode cross sections, Simplified Template Cross Sections (STXS), and their interpretations are presented. Specific scenarios of physics beyond the Standard Model are tested, as well as generic extensions within the framework of the Standard Model Effective Field Theory (SMEFT).

The European Physical Society Conference on High Energy Physics (EPS-HEP2023)
21-25 August 2023
Hamburg, Germany

*Speaker

PoS(EPS-HEP2023)381

1. Introduction

The Higgs boson [1,2] has a rich set of properties that can be verified experimentally, providing powerful tests of the Standard Model (SM) and constraining theories of physics beyond the SM (BSM). The large data sample delivered by the Large Hadron Collider (LHC) [3] at CERN allows measurements of the Higgs boson properties in different kinematic regions.

This paper presents the latest measurements of Higgs boson coupling properties in bosonic decay channels (WW^*, ZZ^*, $\gamma\gamma$), their different production modes cross sections, the signal strength and Simplified Template Cross Section (STXS) measurements, as well as their interpretations in the frameworks of Kappa-κ coupling strength modifiers and the SM Effective Field Theory (SMEFT). The ATLAS [4] measurements are based on full Run-2 p-p collision dataset collected at $\sqrt{s}$=13 TeV with luminosity of 139 fb^{-1}.

2. $H \rightarrow ZZ^* \rightarrow 4l$ STXS Coupling Measurements and Interpretations

The $H \rightarrow ZZ^* \rightarrow 4l$ decay channel (where $l = e$ or μ), is one of the "golden channels" with a fully reconstructable final state and a clean signature. The measurements of three types of Higgs boson coupling properties in this channel are presented analytically in Ref. [5]: (i) The production cross-sections times branching ratio, referred to as cross-sections, for the main production modes in several exclusive phase-space bins in dedicated fiducial regions (ii) Interpretation of the measurements in terms of constraints on the Higgs boson coupling-strength modifiers within the κ-framework and (iii) Interpretation of the measurements in terms of modifications to the tensor structure of Higgs boson couplings using a Standard Model Effective Field Theory (SMEFT) approach.

The measured inclusive cross-section and global signal strength are found in excellent agreement with the SM prediction (p-value 98.6%). The global signal strength, Figure 1(a), is in excellent agreement with the SM prediction: $\mu = 1.01 \pm 0.08$ (stat.) ± 0.04 (exp.) ± 0.05 (th.) = 1.01 ± 0.11. The inclusive $H \rightarrow ZZ^*$ production cross-section, Figure 1(b), for $|y_H| < 2.5$ is measured: $\sigma \cdot B \equiv \sigma \cdot B(H \rightarrow ZZ^*) = 1.34 \pm 0.11$ (stat.) ± 0.04 (exp.) ± 0.03 (th.) pb = 1.34 ± 0.12 pb, in agreement with the SM prediction $(\sigma \cdot B)_{SM} \equiv (\sigma \cdot B(H \rightarrow ZZ^*))_{SM} = 1.33 \pm 0.08$ pb. The cross section measured for each production mode is compatible with SM expectations (p-value of 91%) as shown in Figure 1(b).

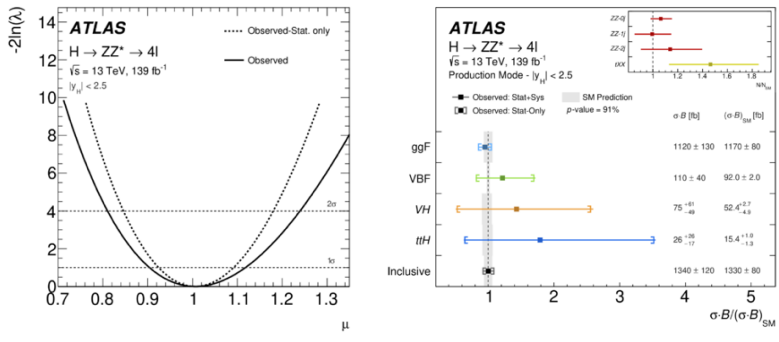

(a) ***(b)***

Figure 1: (a) Observed profile likelihood as a function of the inclusive signal strength μ. ***(b)*** The observed and expected SM values of the cross-sections $\sigma \cdot B$ normalised by the SM expectation $\sigma \cdot B_{SM}$ for the inclusive production and in the Production Mode Stage [5].

In the framework of Simplified Template Cross Sections (STXS), exclusive regions of phase space are defined for each Higgs boson production mechanism, referred to as production bins. They are defined to reduce the dependence on theoretical uncertainties that directly fold into the measurements and at the same time maximise the experimental sensitivity to measure the bins, enhance the contribution from possible BSM effects, and allow measurements from different Higgs boson decay modes to be combined.

All production bins are defined for Higgs bosons with rapidity $|y_H| < 2.5$. Two sets of production bins with different granularity are considered: a) "Production Mode Stage" is defined according to the Higgs boson production modes: gluon–gluon fusion (*ggF*), vector-boson fusion (*VBF*) and associated production with vector bosons (*VH*, where $V = W$ or Z) or top quark pairs ($t\bar{t}H$) b) "Reduced Stage 1.1" is based on the multiplicity of particle-level jets, the Higgs boson transverse momentum p_T^H and the invariant mass m_{jj} of the two jets with the highest transverse momentum. 12 STXS bins measured corresponding to 12 reconstructed categories. The NNs discriminants are used to increase the sensitivity. For Reduced Stage-1.1 bins the results are dominated by the statistical uncertainty, the impact of theory uncertainties is smaller than for the Production Mode Stage. The STXS measurements, as shown in Figure 2(a), agree with SM expectations (p-value of 77%).

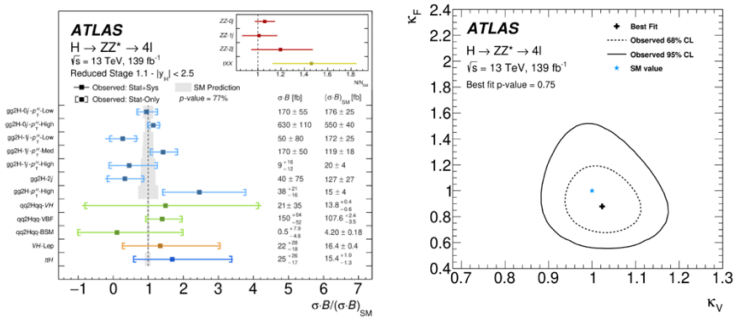

(a) ***(b)***

Figure 2*: *(a) The observed and expected SM values of the cross-sections $\sigma \cdot B$ normalised by the SM expectation $\sigma \cdot B_{SM}$ for the Reduced Stage-1.1 production bins. ***(b)*** Likelihood contours at 68% CL (dashed line) and 95% CL (solid line) in the κ_V–κ_F plane. [5].

The cross-sections measured at the Production Mode Stage are interpreted in the κ-framework, using parameterisations in terms of the coupling-strength modifiers $\vec{\kappa}$ [5]. The coupling-strength modifiers κ_F for fermions and κ_V for vector bosons are defined as $\kappa_V = \kappa_W = \kappa_Z$ and $\kappa_F = \kappa_t = \kappa_b = \kappa_c = \kappa_\tau = \kappa_\mu$. The observed likelihood contours in the κ_V–κ_F plane are shown in Figure 2(b). The best-fit value is $\hat{\kappa}_V = 1.02 \pm 0.06$ and $\hat{\kappa}_F = 0.88 \pm 0.16$, with the correlation of −0.17. The probability of compatibility with the SM expectation is at the level of 75%.

The $H \to ZZ^* \to 4l$ studies in SMEFT aim to set constraints on the tensor coupling structure of Higgs boson couplings in EFT approach. In each production bin, cross sections, BRs and acceptance are parameterized in terms of the Wilson coefficients [5]. The constraints are placed on 5 CP-even and 5 CP-odd (BSM) coefficients, describing interactions of Higgs boson to gluons, top quarks and vector bosons that impact the *VBF* and *VH* production and the Higgs boson decay into Z bosons. The measurements set constraints on one SMEFT coupling assuming a SM value zero on the others. The results are in good agreement with the SM predictions, though dominated by the statistical uncertainty, as shown in Figure 3. The strongest constraint, driven mostly by the

ggF reconstructed event categories, is obtained on the c_{HG} coefficient related to the CP-even Higgs boson interactions with gluons.

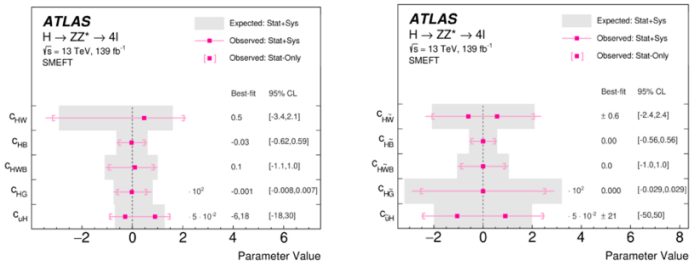

(a) *(b)*

Figure 3: The observed and expected values of SMEFT Wilson coefficients from ***(a)*** CP-even and ***(b)*** CP-odd operators [5].

3. *H→γγ* STXS Coupling Measurements and Interpretations

Despite a small $H\to\gamma\gamma$ branching ratio of (0.227±0.007)%, measurements in the diphoton final state have yielded some of the most precise determinations of Higgs boson properties. The increased integrated luminosity and an improved analysis method allowed the definition of 28 STXS regions. By combining several STXS regions, the analysis [6] provides strong sensitivity to the cross-sections of the main Higgs boson production modes: gluon-gluon fusion (ggF), vector-boson fusion (VBF), and associated production with a vector boson (VH where $V = W$ or Z), or a top quark pair ($t\bar{t}H$). The analysis [6] is specifically optimized for the detection of single-top associated production of the Higgs boson (tH). Two sets of interpretations of these measurements provide constraints on potential effects arising from BSM physics: one in terms of Higgs boson coupling strengths within the κ-framework, and the other in terms of Wilson coefficients describing potential BSM interactions in the context of the SMEFT model.

The inclusive signal strength, μ, is measured by fitting the $m_{\gamma\gamma}$ distributions of the 101 analysis categories to be: $\mu = 1.04\,^{+0.10}_{-0.09} = 1.04 \pm 0.06\,(\text{stat.})\,^{+0.06}_{-0.05}\,(^{\text{theory}}_{\text{syst.}})\,^{+0.05}_{-0.04}\,(^{\text{exp.}}_{\text{syst.}})$. The cross-sections for the main Higgs boson production modes separately are shown with respect to their SM predictions in Figure 4(a). An upper limit at 95% CL on the rate of tH production of 10 (6.8) times its SM prediction is obtained. The 28 STXS measured cross-sections found compatible with their SM predictions, (p-value of 93%), Figure 4(b).

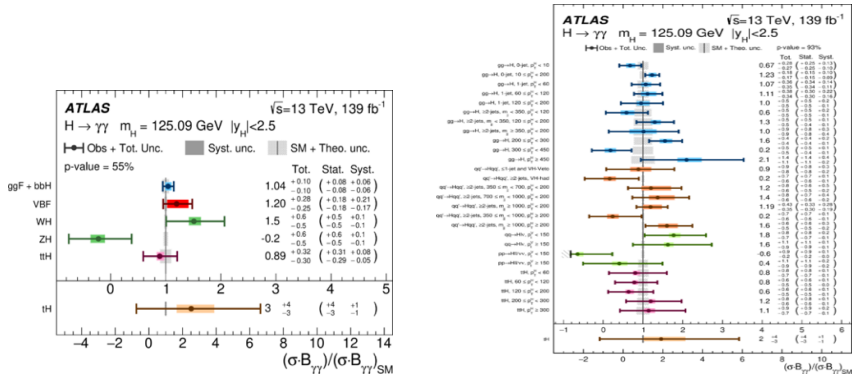

(a) *(b)*

Figure 4: (a) Cross-sections times $H\to\gamma\gamma$ branching ratio for $ggF + b\bar{b}H$, VBF, VH, $t\bar{t}H$, and tH production, normalized to their SM predictions. ***(b)*** Best-fit values and uncertainties for STXS parameters in each of the 28 regions considered, normalized to their SM predictions [6].

Two specific models of coupling modifications are considered [6]. The first model focuses on the κ_t modifier to the Higgs boson coupling with the top quark. Two configurations are used for the $gg \rightarrow H$ and $H \rightarrow \gamma\gamma$ loop processes: a) Both are described using their resolved parameterization as a function of κ_t b) Both are described using the effective couplings κ_g and κ_γ. All other Higgs boson couplings are fixed to their SM values. These two models also allow the sign of κ_t to be probed, with sensitivity coming from interference effects in certain amplitudes. In the second model, the $gg \rightarrow H$ and $H \rightarrow \gamma\gamma$ loop processes are described using the effective modifiers κ_g and κ_γ. Other modifiers are fixed to their SM values.

The measurement in the plane of (κ_g, κ_γ) is shown in Figure 5(a). The best-fit values are found to be $\kappa_g = 1.01^{+0.11}_{-0.09}$, $\kappa_\gamma = 1.02^{+0.08}_{-0.07}$. The negative log-likelihood scans for both configurations are shown in Figure 5(b). In both cases, good agreement with the SM expectation of $\kappa_t = 1$ is seen. When the $H \rightarrow \gamma\gamma$ and $gg \rightarrow H$ loops are resolved, negative values of κ_t are excluded with a significance of 6.7σ or above. When effective loop couplings are used, an exclusion of 2.2σ or above is observed through the sensitivity provided by the tH process, with a smaller contribution from the $gg \rightarrow ZH$ process. Values of κ_t outside of the range $0.87 < \kappa_t < 1.20$ are excluded at 95% CL in the first case ($0.85 < \kappa_t < 1.19$ expected), as are values outside $0.65 < \kappa_t < 1.25$ in the second case ($0.71 < \kappa_t < 1.29$ expected).

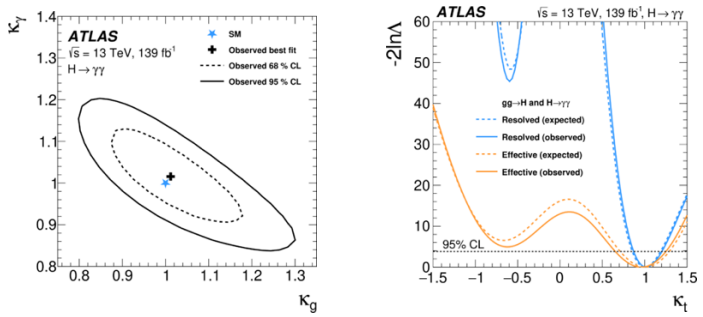

(a) ***(b)***

Figure 5*: *(a) Negative log-likelihood contours at 68% (dashed line) and 95% CL (solid line) in the (κ_g, κ_γ) plane. ***(b)*** Negative log-likelihood scans as a function of κ_t [6].

The SMEFT framework provides a model-independent setting to describe deviations from SM predictions. The Wilson coefficients are considered as the measurement parameters of the model and determined through an interpretation of the STXS results in 33 STXS regions. In the measurements presented [6], one SMEFT parameter at a time is left free to vary, while the others are fixed to 0 as in the SM. Two SMEFT parameterizations are considered: a) Linear and b) Linear plus quadratic. Results are derived using both parameterizations, and their difference is indicative of the impact of the neglected higher-order terms in the SMEFT expansion. The SMEFT parameters are observed in data and no significant deviations from SM predictions is observed.

4. Model Independent Search in $H \rightarrow \gamma\gamma$ + X, Fiducial Cross Section Limits

A model-independent search was performed [7] for excesses in the production rate of the Higgs boson with a mass of 125 GeV in distinct signal regions, defined by the presence and kinematic properties of objects produced in association with the Higgs boson, aiming to set limits

on the BSM production cross section of the Higgs boson in detector-level signal regions. To enable the use of these detector-level cross-section limits in constraining BSM physics models, the detector efficiencies for different signal regions are evaluated [7].

No significant excess beyond the SM expectation was observed, so the $m_{\gamma\gamma}$ distributions in the 22 signal regions are used to set limits on the visible cross section of BSM production using the modified frequentist CLs method. The limits are shown in Figure 6. The observed 95% CL limit on the visible cross section ranges from 0.05 fb ($\geq 3l$) to 0.7 fb ($\geq 4j$).

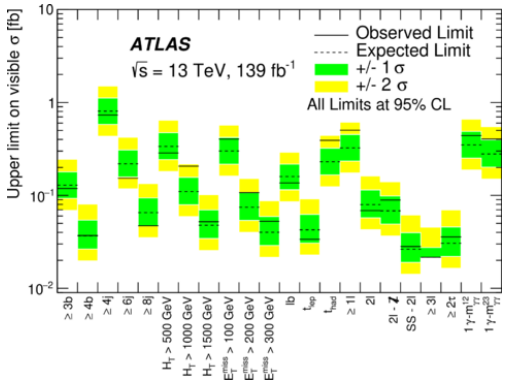

***Figure 6*:** Observed and expected 95% CL limits on the visible cross section of BSM Higgs boson production in each signal region [7].

5. *H→WW* (evμν) ggF+VBF* STXS and Coupling Measurements

The Higgs boson production via gluon-gluon fusion and vector-boson fusion is measured in the $H\rightarrow WW^*\rightarrow e\nu\mu\nu$ decay channel [8], taking advantage of the large branching ratio for $H\rightarrow WW^*$ decay. Cross sections times branching ratios are measured separately for the *ggF* and *VBF* production modes and their combination. Cross-section measurements are also conducted in the Stage-1.2 STXS category scheme. After merging certain STXS bins to ensure sensitivity for all the measured Parameters of Interests (POIs), a total of 11 fiducial cross sections corresponding to different STXS-bound kinematic regions are measured: 6 for ggH production and 5 for EW qqH production, with reconstructed categories based on p_T^H and jet variables.

The cross sections for the *ggF* and *VBF* production modes are determined in the $N_{\text{jet}} = 0$, $N_{\text{jet}} = 1$, and $N_{\text{jet}} \geq 2$ categories. The *ggF* and *VBF* cross sections are the two unconstrained POIs in this fit. A second fit is performed using the same regions but measuring a single POI for the combined ggF and VBF yield. A third fit is made to the STXS regions, where the 11 cross sections measured are POIs. The inclusive measurements were dominated by the systematic uncertainties. All the measurements are observed in agreement with SM predictions.

The cross sections times branching ratio for the ggF and VBF production modes in the $H\rightarrow WW^*$ decay channel, $\sigma_{\text{ggF}} \times B_{H\rightarrow WW^*}$ and $\sigma_{\text{VBF}} \times B_{H\rightarrow WW^*}$, are simultaneously measured to be $\sigma_{\text{ggF}} \times B_{H\rightarrow WW^*} = 12.0\pm1.4$ pb (10.4±0.6) pb, $\sigma_{\text{VBF}} \times B_{H\rightarrow WW^*} = 0.75^{+0.19}_{-0.16}$ pb compared to the SM predicted values of 10.4 ± 0.5 and 0.81 ± 0.02 pb for ggF and VBF respectively. The combined cross section times branching ratio, $\sigma_{\text{ggF+VBF}} \times B_{H\rightarrow WW^*}$, obtained from fitting a single POI, is measured to be $\sigma_{\text{ggF+VBF}} \times B_{H\rightarrow WW^*} = 12.3\pm1.3$ pb compared to the SM predicted value of 11.3 ± 0.5 pb, Figure 7(a). The 68% and 95% confidence level (CL) two-dimensional contours of $\sigma_{\text{ggF}} \times B_{H\rightarrow WW^*}$ and $\sigma_{\text{VBF}} \times B_{H\rightarrow WW^*}$ are consistent with the SM predictions. Figure 7(b) shows a summary of the $H\rightarrow WW^*$ cross sections measured in each of the 11 STXS bins, normalized to the

corresponding SM prediction. The results are compatible with the SM predictions, with a p-value of 53%.

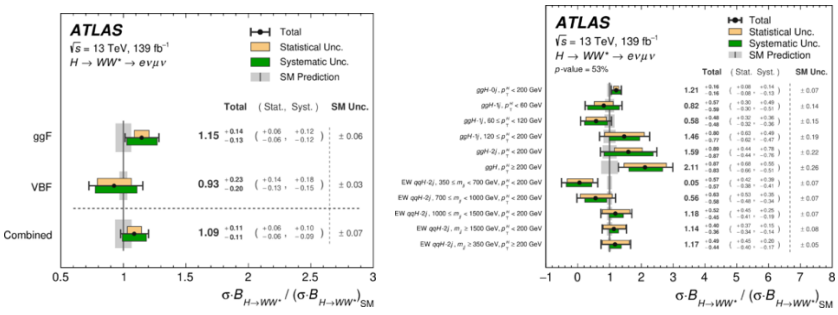

(a) *(b)*

Figure 7: (a) Best-fit values and uncertainties of the $H\rightarrow WW^*$ cross section for the *ggF* and *VBF* processes and their combination, normalized to the corresponding SM prediction. ***(b)*** Best-fit value and uncertainties for the $H\rightarrow WW^*$ cross section measured in each of the STXS bins, normalized to the corresponding SM prediction [8].

6. *VH*, *H→WW*→lνlν*, l*νjj*, *V*: *W*, *Z* Cross Sections Measurements

A measurement of the total Higgs boson production cross sections via associated WH and ZH production using $H\rightarrow WW^*\rightarrow l\nu l\nu$ and $H\rightarrow WW^*\rightarrow l\nu jj$ decays was performed [9] using events with two ($2l$), three ($3l$), or four ($4l$) charged leptons (electrons or muons) in the final state. In the $2l$ channel, both same-sign (SS) and opposite-sign (OS) configurations Is considered, in which the presence of at least one jet and at least two jets required, respectively. In each channel, multivariate discriminants are used to maximise the sensitivity to the Higgs boson signal. The maximum-likelihood fit provides results for the WH and the ZH channels separately and for their combination VH. The VH fit is performed assuming the SM prediction for the relative cross sections of the WH and ZH production processes.

Two fit scenarios are considered: a combined 1-POI fit, where the WH and ZH yields are simultaneously scaled by a single POI, μ_{VH}, and a combined 2-POI fit, where the WH and ZH yields are independently scaled by two POIs, μ_{WH} and μ_{ZH}, respectively. For the combined 1-POI fit, the VH signal strength is measured to be: $\mu_{VH} = 0.92^{+0.21}_{-0.20}$ (stat.)$^{+0.14}_{-0.12}$ (syst.) corresponding to a 4.6σ significance. The total VH cross section times the $H\rightarrow WW^*$ branching ratio is measured to be: $\sigma_{VH} \times B_{H\rightarrow WW^*} = 0.44\pm0.10$ (stat.)$^{+0.06}_{-0.05}$ (syst.) pb, in agreement with the SM expectation: 0.48 ± 0.01 pb. For the combined 2-POI fit, the WH and ZH signal strengths are measured to be: $\mu_{WH} = 0.45^{+0.27}_{-0.25}$ (stat.)$^{+0.18}_{-0.25}$ (syst.) and $\mu_{ZH} = 1.64^{+0.50}_{-0.44}$ (stat.)$^{+0.23}_{-0.17}$ (syst.) corresponding to a 1.5σ and 4.6σ excess. The measurements of the signal strengths of WH and ZH are compatible at a level of 2.1σ. They individually agree with the SM at a level of 1.8σ and 1.2σ, respectively.

The total WH/ZH cross sections times the $H\rightarrow WW^*$ branching ratio are measured to be: $\sigma_{WH} \times B_{H\rightarrow WW^*} = 0.13^{+0.08}_{-0.07}$ (stat.)$^{+0.05}_{-0.04}$ (syst.) pb and $\sigma_{ZH} \times B_{H\rightarrow WW^*} = 0.31^{+0.09}_{-0.08}$ (stat.)±0.03 (syst.) pb. in agreement with the SM expectations: 0.294 ± 0.009 pb and $0.190^{+0.009}_{-0.008}$ pb respectively.

All measurements are consistent with the SM (Figure 8). Figure 8(a) shows the measured values of the total WH, ZH, and VH cross sections times the $H\rightarrow WW^*$ branching ratio, normalised to the SM predictions and Figure 8(b) shows the two-dimensional likelihood contours of the measured values of $\sigma_{ZH} \times B_{H\rightarrow WW^*}$ vs. $\sigma_{WH} \times B_{H\rightarrow WW^*}$ compared with the SM predictions. For the

observed VH combined significance of 4.6σ, the 4l (1-SFOS) is the most sensitive channel. There is strong evidence 4.6σ for $ZH(\rightarrow WW^*)$. The statistical uncertainties are dominant.

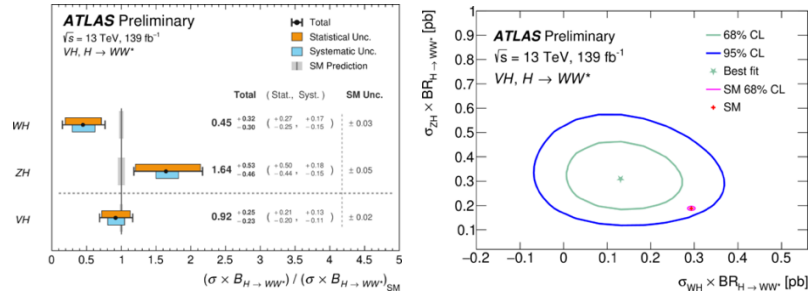

(a) *(b)*

Figure 8*: *(a) Best-fit values of the WH, ZH, and VH cross sections times the $H\rightarrow WW^*$ branching ratio. ***(b)*** 2D-likelihood contours of the measured values of $\sigma_{ZH} \times B_{H\rightarrow WW^*}$ vs. $\sigma_{WH} \times B_{H\rightarrow WW^*}$ for 68% and 95% confidence levels (CLs) compared with the predictions from the SM [9].

7. Conclusions

Analyses of ATLAS Run2 data led to a large improvement on the precision of the Higgs boson couplings and STXS cross section measurements in SM Higgs bosonic channels (WW^*, ZZ^*, $\gamma\gamma$). Interpretations of the cross section and STXS results have been performed in the κ framework and in SM Effective Field Theory. All measurements and their interpretations are consistent with the SM prediction. The results are mostly dominated by statistical uncertainties. Future runs will probe deeper into Higgs properties. The Run3 data at $\sqrt{s}$=13.6 TeV has great potential to improve precision and to probe BSM effects.

References

1. ATLAS Collaboration, *Observation of a new particle in the search for the Standard Model Higgs boson with the ATLAS detector at the LHC*, Phys. Lett. B **716** (2012) 1, arXiv: 1207.7214 [hep-ex].

2. CMS Collaboration, *Observation of a new boson at a mass of 125 GeV with the CMS experiment at the LHC*, Phys. Lett. B **716** (2012) 30, arXiv: 1207.7235 [hep-ex].

3. L. Evans and P. Bryant, *LHC Machine*, JINST **3** (2008) S08001.

4. ATLAS Collaboration, *The ATLAS Experiment at the CERN Large Hadron Collider*, JINST **3** (2008) S08003.

5. ATLAS Collaboration, *Higgs boson production cross-section measurements* and their EFT interpretation in the *4l decay channel at $\sqrt{s}$=13 TeV with the ATLAS detector*, Eur. Phys. J. C **80** (2020) 957.

6. ATLAS Collaboration, *Measurement of the properties of Higgs boson production at $\sqrt{s}$=13 TeV in the H→γγ channel using 139 fb^{-1} of collision data with the ATLAS experiment, JHEP* **07** (2023) 088.

7. ATLAS Collaboration, *Model-independent search for the presence of new physics in events including H→γγ with $\sqrt{s}$=13 TeV pp data recorded by the ATLAS detector at the LHC, JHEP* **07** (2023) 176.

8. ATLAS Collaboration, *Measurements of Higgs boson production by gluon-gluon fusion and vector boson fusion using H→WW*→evμv decays in pp collsions at $\sqrt{s}$=13 TeV with the ATLAS detector, Phys. Rev. D* **108** (2023) 032005.

9. ATLAS Collaboration, *Measurement of the Higgs boson production in association with a vector boson and decaying into WW* with the ATLAS detector at $\sqrt{s}$=13 TeV*, ATLAS-CONF-2022-067.